A position-sensitive detector with lithium glass and MaPMT*

FU Zai-Wei(付在伟)[1,2,3;1)] JIA Ru(贾茹)[4] HENG Yue-Kun(衡月昆)[2,3;2)] QI Ming(祁鸣)[1]
HUANG Chang-Hao(黄长浩)[5] LIU Shu-Lin(刘术林)[2,3] QIAN Sen(钱森)[2,3]
LI Shao-Li(李绍莉)[2,3] CHEN Xiao-Hui(陈晓辉)[2,3] LIU Shu-Dong(刘曙东)[2,3]
LEI Xiang-Cui(雷祥翠)[2,3] HUANG Guo-Rui(黄国瑞)[2,3]

[1] Department of Physics, Nanjing University, Nanjing 210093, China
[2] Institute of High Energy Physics, Chinese Academy of Sciences, Beijing 100049, China
[3] State Key Laboratory of Particle Detection and Electronics, Beijing 100049, China
[4] Physics Department of Huazhong Normal University, Wuhan 430079, China
[5] Siemens Factory Automation Engineering Co, Ltd., Beijing 100016, China

Abstract: A position-sensitive detector is designed for neutron detection. It uses a single continuous screen of a self-made lithium glass scintillator, rather than discrete crystal implementations, coupling with a multi-anode PMT (MaPMT). The scintillator is fast and efficient; with a decay time of 34 ns and thermal neutron detection efficiency of around 95.8% for the 3 mm thick screen, and its light yield is around 5670 photons per neutron and 3768 photons per MeV γ rays deposition. The spatial resolution is around 1.6 mm (FWHM) with the energy resolution around 34.7% by using α (5.2 MeV) rays test.

Key words: lithium glass, detection efficiency, light yield, decay time, MaPMT, spatial resolution

PACS: 29.25.Dz, 29.40.Mc, 29.40.Wk **DOI:** 10.1088/1674-1137/36/11/010

1 Introduction

Neutron position detection is increasingly developed as a powerful tool for evaluating neutron optical devices and nondestructive examinations, and high spatial resolution is desirable in most of the applications, especially neutron crystallography. Moreover, high-intensity is a characteristic of the current pulsed neutron sources, so high detection efficiency, fast response, and position sensitivity are necessary in some cases [1].

It is effective in position detection by using position-sensitive photomultipliers (PSPMTs) coupled with a scintillator, especially in the areas of PET and γ cameras [2, 3]. Researchers usually use the discrete crystal elements coupling with PSPMTs or multi-anode photomultipliers (MaPMTs). The spatial resolution can be set by the crystal dimensions. However, for higher spatial resolutions, narrower crystals are needed, thus problems often pop up like light collection, crystal size control, and high cost [4].

Alternatively, it is worth studying the use of the single continuous scintillator screen coupling with MaPMT, and some application studies are reported for neutron detection [5]. In neutron position detection, a module is usually large, covering even >10 m^2 areas [6], which should possess the high count rate ability and be insensitive to γ rays [6]. Thus it is important to include the kinds and sizes in the scintillator choices.

For a neutron scintillator, LiI is hygroscopic. ZnS:Ag is opaque and its detection efficiency is relatively poor. $Li_6Gd(BO_3)_3$ is promising but it is expensive and sensitive to γ rays. Today, a series of lithium glasses with compositions of MgO has been produced and studied [7]. According to Ref. [6], lithium glass has some good properties. Its light

Received 7 February 2012, Revised 23 March 2012
* Supported by the National Natural Science Foundation of China (10875140, 10890092)
1) E-mail: fuzw@mail.ihep.ac.cn
2) E-mail: hengyk@mail.ihep.ac.cn
©2012 Chinese Physical Society and the Institute of High Energy Physics of the Chinese Academy of Sciences and the Institute of Modern Physics of the Chinese Academy of Sciences and IOP Publishing Ltd

yields are 6000 photons per neutron and 4000 photons per MeV γ rays energy deposition. Its detection efficiency and response speed are also better than the ZnS:Ag/^{6}LiF. However, the compositions of lithium glass may result in different scintillation properties. Lithium glass without MgO [8] has been reported for a long time, but few papers have studied its specific properties. Thus it is essential and useful to study the properties of lithium glass.

In this paper, lithium glass without MgO has been made, and its light yield, detection efficiency, and decay time are studied. Using this kind of scintillator, a position sensitive detector is made by using MaPMT (H8500). Unlike many reports, we choose a single continuous lithium glass scintillator screen rather than the discreet crystal implementations. The position response of the MaPMT is studied by an LED spot, and the spatial resolution of the detector is preliminarily studied by using a collimated α ray (^{239}Pu) with the energy of 5.1 MeV, which is approximate to the reaction energy of ^{6}Li(n,α)^{3}H around 4.8 MeV.

2 Detector overview

The position sensitive detector consists of a MaPMT, a light guide scintillator screen, a reflector, and an electronic system. There are two kinds of lithium glass scintillator screens with the thickness of 1 mm and 3 mm, and all the scintillator screens are cycled with the same diameter of 5 cm. The glass components are listed in Table 1. The materials with mass density of 2.31 g/cm^3 contains lithium elements around 6% in weight, and the abundance of ^{6}Li is 90%.

Table 1. Lithium glass compositions.

composition	SiO_2	Li_2O	Al_2O_3	Ce_2O_3
weight fraction	74.32%	13%	7.52%	5.16%

The MaPMT has 8×8 pixels corresponding to 64 channels readout with 12 stages of metal channel dynodes, and the last dynode signal offers the common trigger in experiments. The cross section is around 52 mm×52 mm, each pitch is 6 mm×6 mm, but the active photo cathode area is 49 mm ×49 mm, and the effective pitch size is around 5.8 mm×5.8 mm. The light guide is a piece of organic glass with the thickness of 1 mm greased with oil on both sides. It is placed between the MaPMT and the scintillator screen in the experiment. Here the resistive chain circuit shown in Fig. 1 is employed to simplify readouts to four channels of A, B, C, and D. In experiment, MaPMT works with the high voltage of 840 V, and each signal of A, B, C, and D is amplified by ten times with a fast amplifier (caen, N978), and then sent into a QDC (V792, caen) to record the output charges event by event, via which each position (x, y) is acquired by the equations

$$x = \frac{Q_{\rm a}+Q_{\rm b}}{Q_{\rm a}+Q_{\rm b}+Q_{\rm c}+Q_{\rm d}}, \quad (1)$$

$$y = \frac{Q_{\rm a}+Q_{\rm d}}{Q_{\rm a}+Q_{\rm b}+Q_{\rm c}+Q_{\rm d}}. \quad (2)$$

Where $Q_{\rm i}$ (i = a, b, c, d) is the charge corresponding to the A, B, C and D outputs respectively.

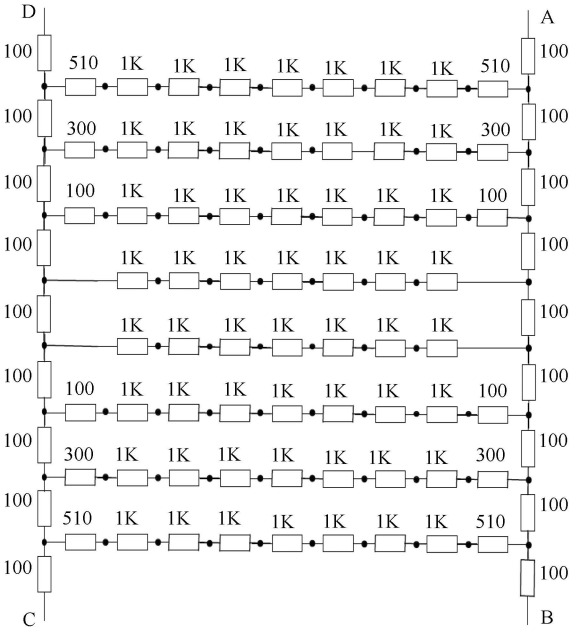

Fig. 1. The resistive chain circuit readout for MaPMT.

In order to get high signal-to-noise ratio and high spatial resolution, efficient light collection should be designed for the detector. Here, a back reflector of Tyvek film on the top of the screen is selected to direct scintillation light into the MaPMT as much as possible, while preserving the scintillation light spatial localization. And in this paper, the preliminary tests used collimated α rays (^{239}Pu), whose collimation channel is a hole with radius of 1 mm.

3 Scintillator screen properties

The light yield of the scintillator determines the value of $Q_{\rm i}$ (i=a, b, c and d), which consequently determines the spatial resolution. And the scintillator detection efficiency and decay time directly determine

the whole detector performances. Thus knowledge of the scintillator properties is necessary.

3.1 Lithium glass decay time

Decay time governs how frequently the scintillator can be achieved. The influences become increasingly important when the detector works under an intensive neutron pulse, in which the long decay time is likely to cause the signal piling up and a bad signal-to-noise ratio.

In order to acquire the time properties, the lithium glass is coupled with a PMT (XP2020) and irradiated by a neutron source of ^{252}Cf, and Fig. 2(a) shows the eight pulse shapes whose mean wave is displayed in Fig. 2(b). For the mean wave, the time width at the $\frac{1}{e}$ time of the pulse height is around 37 ns, and the corresponding decay time is around 34 ns.

3.2 Light yield

We measured the scintillator light yield by the 3 mm thick screen with a moderated ^{252}Cf neutron source (in thermal range, flux 1–2 Hz/cm^2) and ^{137}Cs source respectively. The screen, greased with silicon oil, is coupled with a PMT (XP2020) with the gain of 1.2×10^7, and the PMT is sensitive for single photoelectron. Tyvek film is employed for the packages in order to collect the scintillation light as much as possible. The PMT output is directly sent into an oscilloscope (Lecroy Wave Pro 7100) to record the pulse shape with the sampling frequency of 10 GHz.

The charges of the PMT outputs are derived from integrating the amplitude in a period of 400 ns for both excitations of ^{252}Cf and ^{137}Cs source. The flux of the neutron source is around 1–2 Hz/cm^2 and the activity of ^{137}Cs source is around 1×10^6 Bq. Fig. 3 shows the results of the charge distribution for both radiation sources, in which the negative channel indicates the integral value for electrons charge.

For ^{137}Cs excitation, charge distribution (solid curve) does not have a clear peak. The Geant4 simulation reveals that the ^{137}Cs energy deposition is around 433 keV in the 3 mm thick screen. In Fig. 3, the neutron spectrum (dot curve) shows two charge quantity peaks, the lower one around 30 pC, and the other one is centered with the channel of 880 pC. Obviously, the pedestal is about 30 pC, and there is good separation between the pedestal and the neutron signal. The light yield is estimated around 5671 photons per neutron, and 3768 photons per MeV γ energy deposition.

3.3 γ suppression capability and detection efficiency

The γ suppression capability is an important parameter for neutron detection, especially for the scintillation detector. It is necessary to acquire the γ suppression (ξ) along with its corresponding neutron detection efficiency. The lithium glass γ suppression capability can be defined as the ratio of the recorded γ rays counts (C_γ) above a given threshold and the total γ rays counts in the experiment,

$$\xi = \frac{C_\gamma}{\text{total } \gamma \text{ counts}}; \tag{3}$$

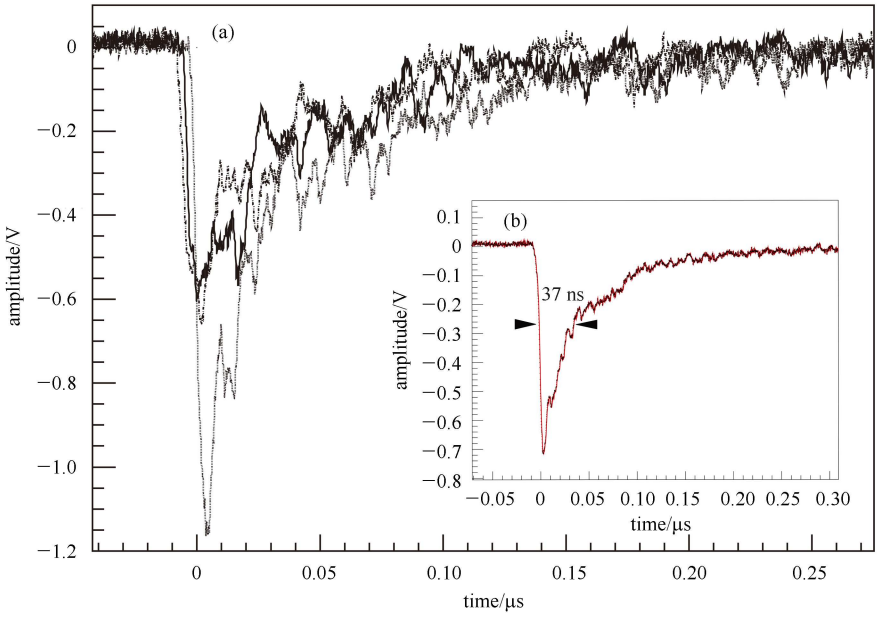

Fig. 2. The lithium glass neutron pulses and decay time.

and its corresponding neutron detection efficiency is defined as

$$\Xi = \frac{C_{\rm n}}{\text{total neutron counts}}. \quad (4)$$

Here $C_{\rm n}$ is the counts of neutron pulses with amplitude larger than the given threshold.

In experiment, we use the 3 mm thick lithium glass to measure the γ suppress capability with a γ radiation source of ^{137}Cs (661 keV). Because the activity of ^{137}Cs is so large that the number of γ triggers far more than that of the noise triggers, thus the noise trigger can be ignored. At last, the total γ counts are 7598. For the neutron test, the pedestal charge is less than 50 pC as shown in Fig. 3, and the total neutron counts are 2803.

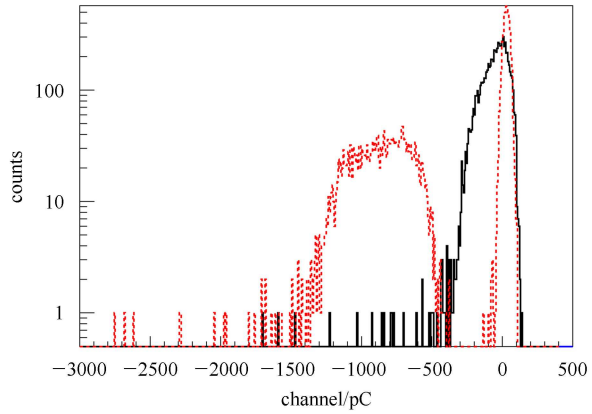

Fig. 3. The charge distribution of 3 mm thick lithium glass under ^{252}Cf and ^{137}Cs excitation. The dot curve is for neutron the test and the solid curve is for the ^{137}Cs test.

Table 2 shows the measured γ suppression capabilities and the neutron detection efficiencies varying with different thresholds. The γ suppression capability becomes better as the threshold increases, and its value at the threshold of 1100 pC is about 5×10^4 with the neutron detection efficiency of 14.8%.

Table 2. The parameters of ξ and Ξ varying with thresholds measured with ^{252}Cf and ^{137}Cs.

threshold/pC	$C_{\rm n}$	C_γ	$\xi(\times10^{-3})$	$\Xi(\%)$
50	2803	3423	450.6	100
100	2796	2091	275.2	99.8
150	2795	1152	151.6	99.7
200	2795	522	68.7	99.7
300	2795	63	8.3	99.7
500	2763	17	2.2	98.6
555	2684	15	1.8	95.8
600	2558	13	1.7	91.26
900	1179	6	0.8	42.1
1100	415	4	0.5	14.8

Supposing Ξ_1 and Ξ_3 are the efficiencies of the screens of 1 mm and 3 mm thick screens respectively, and assuming the attenuation length of scintillation light in the glass scintillator is longer than the screen thicknesses. The relationship between the Ξ_1 and Ξ_3 can be derived from the probability principles,

$$\Xi_3 = 1-(1-\Xi_1)^3. \quad (5)$$

At the threshold of 555 pC, the γ suppression capability for 661 keV γ rays is 1.8×10^{-3}, and its corresponding neutron detection efficiency is 95.8%. Thus, the neutron detection efficiency of lithium glass with the thickness of 1 mm can be calculated from Eq. (5) about 65.2% at this threshold.

A Geant4 simulation shows the capture efficiencies of the two screens at the neutron energy of 0.025 eV are 67.0% and 96.2% for the 1 mm thick and the 3 mm thick screens, respectively. The results are consistent with the measurements.

4 Spatial resolution test

4.1 Position response of MaPMT

The anodic undersampling perhaps exist because of the pixelated anodes. Thus the linearity of the MaPMT should be examined in experiment.

We use an LED to light a fiber with the radius of 1 mm, and the fiber with step of 2.5 mm along the X-axis gives a light spot close to the face of MaPMT. The position response of the MaPMT is shown in Fig. 4, in which the X-axis is scaling the real positions and the Y-axis is scaling the signal calculating positions. It shows that there are obviously three stepwise corresponding to the anode structures, and it indicates that the electrons did not experience enough spread in the multiplication process. Such nonlinearity can be corrected by using the light guide, which ensures that the scintillation light disperses enough and is sampled by several anodes. In our experiment, we use organic glass with a thickness of 1 mm as our light guide.

4.2 Screen thickness effects

Screens of different thicknesses cause the detector to vary in terms of detection efficiency, the light transmission, and the spatial resolution. Usually, one has to make a compromise between such parameters. Here, we test the detector spatial resolution using the two scintillator screens of 1 mm and 3 mm in thickness. Actually, the detection efficiencies of both of

the two thick screens are fairly high for general experiments. Thus, We should choose one for better spatial resolution and test the whole detector performances for position detector.

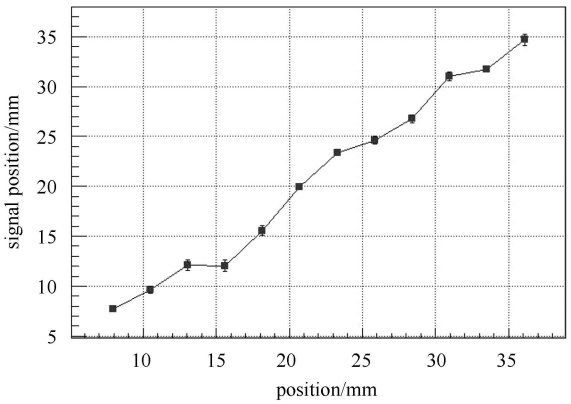

Fig. 4. The position response with 1 mm diameter light spot along X-axis.

Figure 5 shows the MaPMT front face, the numbers from 1 to 64 represent the 8×8 pixel indexes. Here we choose the central pixels No. 28, 29, 36 and 37 as the objects of studying the thickness effects for the spatial resolution. The back reflector has a 1 mm hole to let the collimated α rays radiate on each object pixel center. Table 3 and Table 4 are the standard deviations along the X-axis and Y-axis, respectively, which correspond to the position distributions of pixel Nos. 28, 29, 36, and 37. Screen 1 and Screen 3 represent the lithium glass with thickness 1 mm and 3 mm, respectively.

Table 3. The center pixels spatial resolution (σ_X) for the two different thickness scintillators.

screen	No. 28/mm	No. 29/mm	No. 36/mm	No. 37/mm
1	1.22	1.11	1.05	0.96
3	1.29	1.38	1.24	1.21

Table 4. The center pixels spatial resolution (σ_Y) for the two different thickness scintillators.

screen	No. 28/mm	No. 29/mm	No. 36/mm	No. 37/mm
1	1.12	1.08	1.22	1.02
3	1.27	1.15	1.22	1.20

Obviously, each screen can get a good resolution of below ∼3 mm(FWHM) and even better than 2.3 mm (FWHM). In addition, the tables also express that the thinner the screen, the better the spatial resolution. Thus we choose the screen with a thickness of 1 mm for the position-sensitive detector.

1	2	3	4	5	6	7	8
9	10	11	12	13	14	15	16
17	18	19	20	21	22	23	24
25	26	27	28	29	30	31	32
33	34	35	36	37	38	39	40
41	43	43	44	45	46	47	48
49	50	51	52	53	54	55	56
57	58	59	60	61	62	63	64

Fig. 5. The front face of MaPMT H8500.

5 Result and discussion

From Table 3, the FWHMs of position distribution along X-axis of 1 mm thick screen are from 2.3 mm to 2.9 mm. We thus choose 8 test points with the adjacent distances from 2.3 mm to 3.0 mm to study the separation and position linearity. The specific adjacent distances D are listed in Table 5, in which the unit of D is millimeter.

Figure 6 (a) shows the image of the 8 points, which are able to distinguish each other clearly. In Fig. 6(b), it shows 8 Gauss distributions of the 8 points and corresponding mean values corresponding to the positions calculated from the signals. The right axis is the real position of the 8 points along X-axis. Thus we can study the position linearity by fitting the 8 points by a line, and the fitted parameters are displayed on the right upper panel. It shows that the points are good in linearity. On the left upper panel of Fig. 6(b), it shows the Gauss fit of X distribution of Point 3 marked in Fig. 6(a), its σ value is around 0.67 mm(or FWHM 1.6). Because the reaction energy of ^{6}Li(n,α)^{3}H is approximate to the α energy, we can suppose the two light yields are approximate. Thus, a good spatial resolution can be expected by neutron.

Table 5. The test points adjacent distances along X-axis.

	1→2	2→3	3→4	4→5	5→6	6→7	7→8
D/mm	2.6	2.7	2.6	3.0	2.3	2.7	2.8

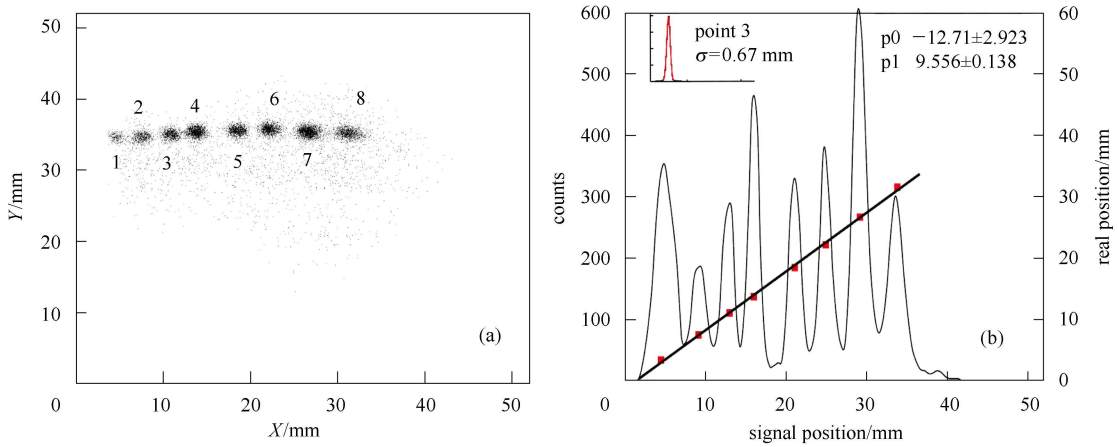

Fig. 6. (a) The 8 test points scattering plot of X and Y; (b) the position projects on X-axis corresponding to (a) and the position linearity.

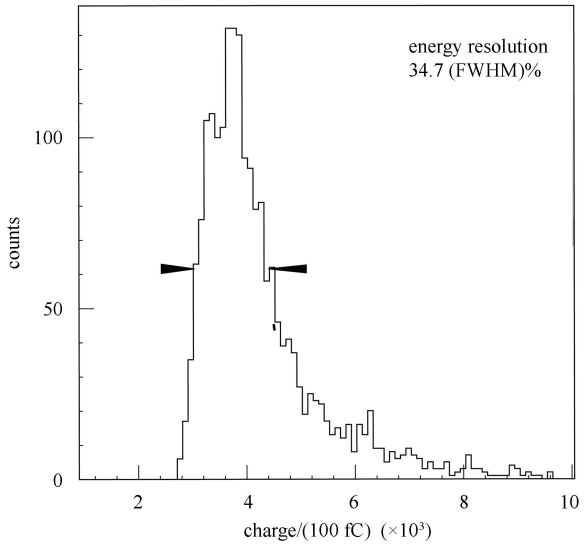

Fig. 7. The spatial resolution of Point 3.

Figure 7 shows the energy distribution of the detector, which is derived from the sum of $Q_{\rm i}$ (i = a, b, c, d) and the FWHM is around 34.7%. The energy resolution is a little larger, perhaps because the transparency of the glass we made is not too good.

6 Conclusion

A position-sensitive detector has been developed based on a self-made lithium glass scintillator screen coupling with MaPMT. The scintillator properties have been studied, and the results show its light yields around 5671 photons per neutron and 3768 photons per MeV γ rays deposition. The lithium glass decay time is around 34ns with neutron excitation, and its detection efficiency can achieve around 65.2% and 95.8% for the thicknesses of 1 mm and 3 mm, respectively. The γ suppression capability of 3 mm thick lithium glass is around 1.8×10^{-3} for 661keV γ rays with the neutron detection efficiency of 95.8%. Then, we studied the detector position responses under the α rays excitation, including the thickness of the scintillator screen effects, the position linearity, spatial resolution, and energy resolution. It shows that a 1 mm thick screen can achieve good position linearity and a high spatial resolution of 1.6 mm (FWHM) with an energy resolution of around 34.7% (FWHM).

We wish to thank LI Dao-Wu of IHEP for his useful discussion.

References

1 Van Eijk C W E, Bessiere A, Dorenbos P. Nucl. Instrum. Methods A, 2004, **529**: 260–267
2 Nishimura H, Hattori K, Kabuki S et al. Nucl. Instrum. Methods A, 2007, **573**: 115–118
3 Pani R, Pellegrini R, Cinti M N et al. Nucl. Instrum. Methods A, 2003, **505**: 590–594
4 Siegel S, Cherry S R, Ricci A R. IEEE Trans. Nucl. Sci. 1995, **42**(4): 1069–1074
5 Sakai K, Hirota K, Adachi T et al. Nucl. Instrum. Methods A, 2004, **529**: 303–306
6 van Eijk C W E. Nucl. Instrum. Methods A, 2001, **460**: 1–14
7 BAN G, Bodek K, Lefort T et al. Nucl. Instrum. Methods A, 2009, **611**: 280–283
8 JI Chang-Song. Handbook of Nuclear Radiation Detection and Their Experiment Techniques. first edtion. Beijing: Atomic Energy Press, 1990. 324 (in Chinese)